Sensing in Electroanalysis

Vol. 7 (K. Kalcher, R. Metelka, I. Švancara, K. Vytřas; Eds.), pp. 29–56.

ISBN 978-80-7395-563-2 (printed); 978-80-7395-564-9 (on-line)

Photolithographically Fabricated Microelectrodes with Interacting Diffusion Layers: Fundamentals and Basic Applications

Peter Tomčík*

Department of Chemistry, Faculty of Education, The Catholic University in Ružomberok, Hrabovská cesta 1, Ružomberok SK - 034 01, Slovak Republic.

Abstract: This book chapter describes photolithographically fabricated microelectrodes and their arrays as very perspective tool in contemporary electrochemistry. Photolithographic thin layer technology allows to fabricate an array of sensors of micrometric dimension separated with a very small gap. This fact enables an overlapping of diffusion layers of single microelectrodes as members of the array. Various basic types of microelectrode arrays with interacting diffusion layers are described and their analytical abilities are accented. Theoretical approaches of diffusion layer overlapping and consequences of close constitution effects such as collection efficiency and redox cycling are discussed. Examples of basis applications in electroanalytical chemistry such as amperometric detectors in HPLC and substitutional stripping voltammetry are also given.

Keywords: Photolitography; Interdigitated microelectrode arrays; Microband electrodes; Collection efficiency; Redox cycling; Substitutional stripping analysis; Detection of catecholamines; Neurotransmitters.

*) Author to whom correspondence should be addressed. E-mail: peter.tomcik@ku.sk

Introduction

During research on microelectrodes, it was shown that the decrease of a characteristic dimension of the working electrode to the value comparable with the electrode diffusion layer thickness results in advantages for electrochemical measurements [1,2]. High density steady-state diffusion of electroactive species towards the microelectrode surface [3,4], low capacity of electric double layer [5,6], current measurable also in 2-electrode arrangement with a small amount of supporting electrolyte [7,8] and high signal-to-noise ratio [9,10] make micro-electrodes efficient devices for applications in trace analysis [11,12] and microanalysis [13,14].

However, diffusion current magnitudes are relatively low due to small microelectrode area [15,16] causing such problems during measurement of the microelectrode response [17]. One way how to overcome this main disadvantage of microelectrodes and save their powerful properties is coupling them to arrays.

In this time, a subject of intensive research are microelectrode systems where single microelectrodes are each other placed in a very small distance allowing an overlapping of their diffusion layers. Close geometrical constitution is a starting point of some effects bringing significant benefits in the electroanalysis of electroactive and electroinactive species. These effects could be reached not only by a polarization of each electrode in the array with the same potential, but also by a polarization of individually addressable microelectrodes with various potentials performed by multipotentiostat.

Electroactive species generated on one microelectrode (generator segment of array) may diffuse across the small gap towards second microelectrode (collector segment of array) where they can be electrochemically detected. As in the case of rotating ring disc electrode a collection efficiency could be defined, however substantially higher value can be achieved for microelectrode array with suitable geometry due to non convective mass transport to the microelectrode array surface. If on the collector an original analyte is formed due to concentration deficit diffuses back to generator and may oxidize/reduce again causing such redox cycling effect which enhances current without capacity noise increasing such sensitivity and selectivity of electrochemical analysis.

Theory of Mass Transport at Microelectrode Arrays

Theoretical studies [18] are focused on chronoamperometry [19] and linear sweep voltammetry [20] at microelectrode arrays consisting microcylindrical and microband electrodes [21]. For diffusion layer thickness of microband electrode can be derived,

$$\delta = \frac{zFADc}{I} \tag{1}$$

where "z" is the number of electrons taking place in electrode reaction, "F" Faraday constant, "A" microelectrode area, "D" diffusion coefficient, "c" concentration of electroactive species in the bulk phase of analyzed solution, and "I" diffusion current. However, due to small characteristic diameter of microelectrode a spherical (nonlinear diffusion) should be taken into account, therefore the diffusion current can be expressed as,

$$I = \frac{zFAcD^{1/2}}{\sqrt{\pi t}} + \frac{zFcDP}{2} = I_{Cott} + \frac{zFcDP}{2} \quad (2)$$

where "t" is duration of experiment and "P" is parameter. Very important characteristic parameters for microband electrode are its width, W_e, and length, L [22]. Considering those facts, Aoki [23] has derived an equation for diffusion layer thickness of microband electrode in a dimensionless time domain,

$$\Theta = \frac{Dt}{W_e^2} < 10^8 \quad (3)$$

where "W_e" is microelectrode width:

$$\delta = \frac{W_e}{\frac{1}{\sqrt{\pi\Theta}} + 0.97 - 1{,}10\exp\left[\frac{-9.90}{\left|\ln(12.37\Theta)\right|}\right]} \quad (4)$$

From this equation is apparent that diffusion layer width is growing with time and is lower than calculated from Cottrell equation due to edge effect [24]. For very short times diffusion layer thickness becomes equal to calculated from Cottrell equation. When the time is sufficiently long a steady-state current is reached and voltammogram recorded at low scan rate will have a sigmoidal shape [25]. Diffusion layer thickness grows with microelectrode width W_e [26]. When the microelectrode is thinner (low W_e) the time change of δ is higher and lower times are needed for the obtaining steady-state currents [27].

Diffusion layer overlapping at microband arrays of electrodes

For the pictorial description of the overlapping diffusion layers of the array containing microband electrodes, three cases should be distinguished:

1. When $\delta < W/2$, where $W=W_e+W_g$ and W_g is a gap width between two adjacent microelectrodes, there is no diffusion layer overlapping and the total current of microelectrode array is equal to the current sum of all microelectrodes coupled in the array:

$$I_{total} = mI \quad (5)$$

where "m" is number of single electrodes in the array, when the current, I, can be calculated from the equation (2).

2. When $\delta > W/2$ diffusion layers of two adjacent microelectrodes are partially overlapped. Ju [28] suggested for quantitative consideration of microband electrodes overlapping angle Ψ (figure 1.)

$$\Psi = \tan^{-1}\left(\frac{[\delta^2 - (W/2)^2]^{1/2}}{W/2}\right) \tag{6}$$

For long electrolysis time angle Ψ and diffusion layer thickness are growing, however the microelectrode area is lower, therefore diffusion current magnitude is lower in comparison with a case 1. Equation (7) offers good results in a time domain $\theta < 10^8$ in which time dependent two dimensional diffusion is taking into account as well as the microelectrode has a sufficient length to not consider the edge effect on its both ends,

$$I_{total} = mzFDcL\left[\frac{1}{\pi\Theta} + 0.97 - 1.10\exp\left(-\frac{9.90}{\ln(12.37)}\right)\right]K \tag{7}$$

where

$$K = 1 - \frac{2}{\pi}\tan^{-1}\sqrt{\frac{4W_e^2}{\left[\frac{1}{\sqrt{\pi\Theta}} + 0.97 - 1.10\exp\left(-\frac{9.90}{|\ln(12.37)|}\right)\right]^2 W - \frac{W^3}{4}}} \tag{8}$$

3. If the angle Ψ reaches a limiting value $\Psi = \delta/2$, diffusion layers are totally overlapped. For total current an equation has been derived

$$I_{total} = \frac{mzFcD(W_e + W_g)L}{\sqrt{\pi Dt}} \tag{9}$$

where L is length of one microelectrode in the array.

The quantification of diffusion layers overlapping could be also described by an overlapping factor

$$S = 1 - \frac{I_{total}}{\sum_{j=1}^{m} I_j} \qquad (10)$$

where I_j is current of j electrode when others are disconnected from multipotentiostat. Overlapping factor usually represents a ratio of diffusion layer area of overlapped electrode to the whole area of diffusion layers other individually addressable microelectrodes in the array. It depends on time (experiment duration) as well as on the geometrical arrangement of microelectrodes in the array.

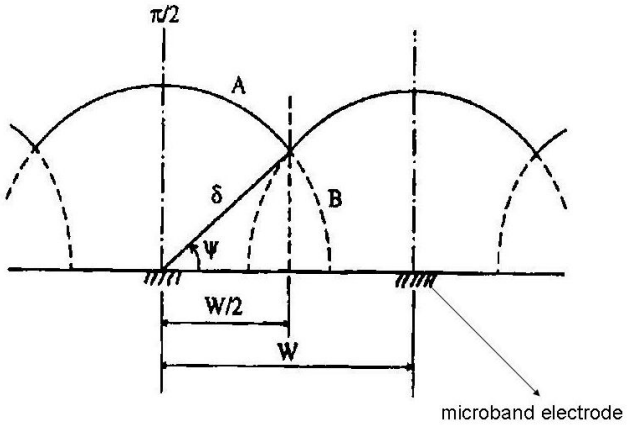

Fig. 1. : *Cross section model of diffusion layers overlapping for microband electrode [28]*

Voltammetric Studies on Interdigitated Microelectrode Arrays

Interdigitated microelectrode arrays (IDA) have more advantageous geometry in comparison to microband electrodes [29-31]. Chronoamperograms on various types of IDA has been measured using ferocen in acetonitrile solution as testing system.

Generator current in dual (bipotentiostatic) mode reaches steady-state in 100 ms. This time is needed for species to diffuse through the gap to create concentration gradient. Shorter time for reaching steady-state current of 10 ms can be obtained in the case when IDA microelectrodes with submicrometrical gap are used [32] which is important in analysis of compounds with a short life. Second advantage of IDA microelectrodes in dual mode is that chronoamperograms measured on collector do not contain capacity current which represents a noise.

Equation of chronoaperometric curve was derived by Aoki [33,34] and Coen [35] based on these prerequisites:

1. Number of metal microbands of IDA array is sufficiently high to not count the edge effects
2. The width of each metal microband W_e is the same
3. The metal layer length L is many times greater than W_e
4. The transport of electroactive species towards the IDA microelectrode surface is made by diffusion only.
5. Diffusion coefficients are equal for both redox forms of analyzed electrochemical system

The current is similarly as in the case of microband electrode function of dimensionless Aoki time θ

$$\frac{I}{LzFDc} = \frac{5.553}{\ln(4\Theta)} - \frac{6.791}{\ln(4\Theta)^2} \qquad (11)$$

In ref. [36], the results calculated from equation (11) and Cottrell equation were compared with chronoamperograms measured in dual and single (monopotentiostatic) mode on IDA electrode with a microband width of 3μm and the gap of 2μm. Currents were divided by number of metal microbands and normalized by current of single microbands.

It was shown that current in single mode is higher than current calculated from Cottrell equation, however it is lower than current calculated from equation (11) due to shielding effect [34]. Current in dual mode is higher than calculated from Aoki-Coen equation because of redox cycling. When the gap between two adjacent metal microbands in IDA microelectrode is increased the current in single mode will be higher because of diffusion layer overlapping is decreased, but, in the dual mode, the current is decreased due to lower redox cycling. When collector is polarized with a constant potential and cyclic voltammogram is measured on generator, collector current is capacity noise free even at high scan rates around 10 000 $mV.s^{-1}$ [36]. A slight hysteresis on collector voltammogram (fig.3) is caused by interruption between generating and collecting processes. Potential difference between cathodic and anodic collector wave is around 80 mV corresponding to time response of 8 ms. This time is needed for the transfer of electroactive species from generator to the collector across the gap.

In a classic voltammetric experiments capacity current grows with a scan rate and faradayic with its square root. At high scan rates voltammetric signal becomes unclear due to high charge current. It can be subtracted but signal is deformated by ohmic drop. This problem may be solved by IDA microelectrode with short time response allowing extremely short electrolysis during recording of the respective cyclic voltammogram and investigations on fast kinetics processes.

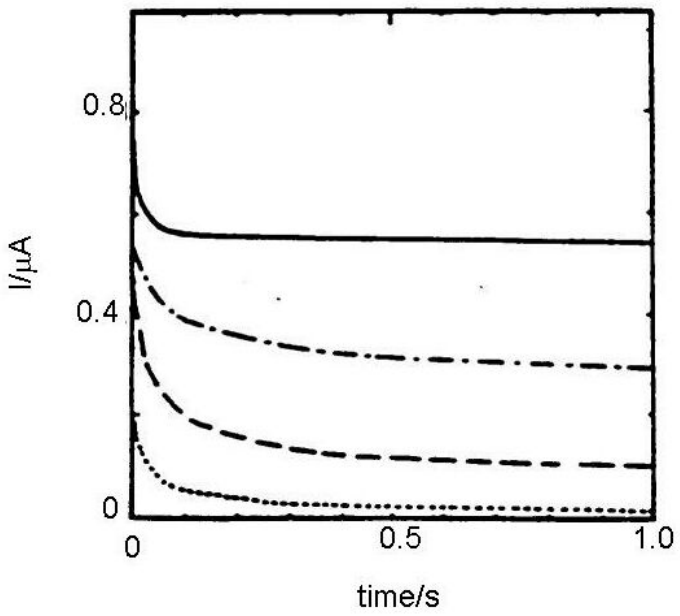

Fig. 2.: *Chronoamperograms of 1 mmol.dm^{-3} ferocene solution in acetonitrile with ammonium tetrafluoroborate on IDA array containing 50 pair of microbands with a gap of 2μm and metal layer width of 3 μm. [36].* All results were normalized by dividing number of microbands, (—) generator current in dual mode, (— —) generator current in single mode, (¯·¯·¯·¯} calculated from Aoki-Coen equation, (.....) calculated from Cottrell equation.

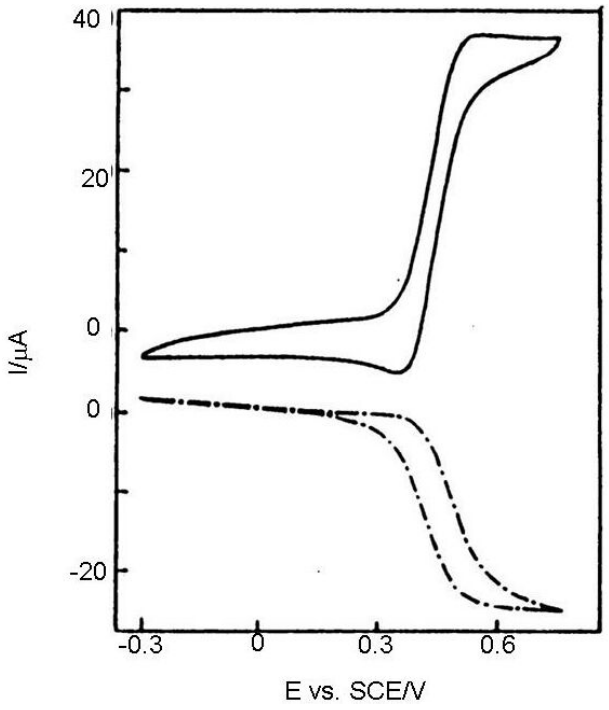

Fig. 3.: *Generator and collector cyclic voltammogram at the same IDA and solution as on Fig. 2 at 10 000 V/s [36].*

Collection Efficiency and Redox Cycling as Consequences of Microelectrode Arrays Diffusion Layer Overlapping

Collection efficiency is usually calculated as collector to generator current ratio. Bard et all [36] showed that the collection efficiency depends above all on the gap between collector and generator segment of each microelectrode array and can be expressed by the equation,

$$\Phi = 0.095 + 0.33\log j_{gap} - 0.035(\log j_{gap})^2 \quad (12)$$

where: $j_{gap} = 4Dt / (W_g)^2$

Collection efficiencies of microelectrode arrays with various geometrical arrangements were compared. On the base of this comparison following conclusions were summarized:

1. Collection efficiency depends not only on the gap between two individually addressable segments of microelectrode array, but also on the microelectrode width.
2. For various electrochemically reversible species with various diffusion coefficients very small change in collection efficiency was observed, therefore collection efficiency is crucially influenced above all by geometrical factors.

Linear dependence of parameter W_e / $4+W_g$ on square root of time (chronoamperogram duration) was observed for the case when current reaches 50% of limiting diffusion current. Above mentioned parameter represents an average diffusion length between generator and collector and is very suitable for evaluation of collection efficiency on geometrical factors especially for IDA microelectrode arrays [37].

These facts are analogous to rotating ring-disc electrode (RRDE) used in electroanalytical chemistry for detection of electroinactive species by a diffusion layer titration. The analog to an inverse value of W_g is angle rate ω. Current response of RRDE is enhanced by analyte convection during hydrodynamically stable conditions. Collection efficiency on the ring is usually less than 50 % and is substantially lower as for vertically separated IDA micro-electrode array reaching at least 95% or higher. Additional disadvantage of RRDE vs. IDA is high noise related to brush contacts. Other substantial difference between RRDE and IDA is interrelationship of diffusion layers. In the case of RRDE, only diffusion layer of ring is influenced by the disc electrode reaction due to centrifugal movement of analyte in a

close vicinity of rotating body of the electrode; therefore, the ring will never serve as a generator [38-40].

The second interesting feature of microelectrodes with interacting diffusion layers is redox cycling [41]. This phenomenon occurs when on one microelectrode (generator) is electroactive and electrochemically reversible redox species generated. After diffusion across the gap it is amperometrically detected on the second microelectrode with a potential corresponding to the opposite electrode reaction to the generator one (dual mode). Generator and collector currents are both steady-stated and the generator current is several times higher as in the case when collector microelectrode is disconnected from potentiostat (single mode). This is also called as forced redox cycling. Unpotentiostated microelectrode in a close vicinity to generator does not influence its response and behaves as insulator. When linear sweep voltammogram is recorded at very slow scan rates (less than 5 $mV.s^{-1}$) a quasi steady-state wave is obtained however its height is several times lower in comparison during using suitably polarized collector microelectrode.

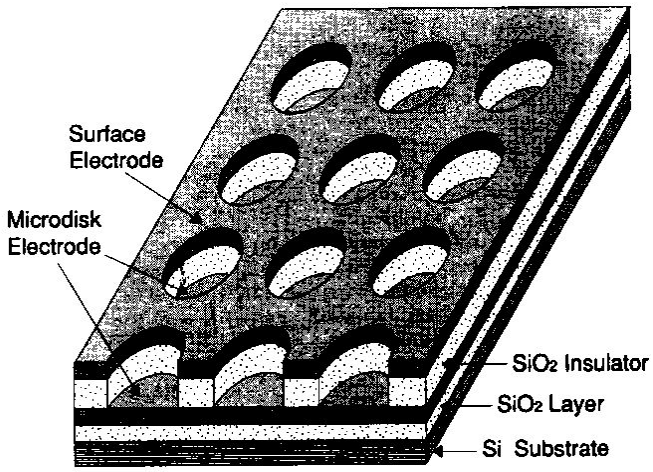

Fig. 4: *Microdisc array with vertically separated macroelectrode [42]*

If macroelectrode with significantly greater area is placed into diffusion layer of microelectrode which generates electrochemically reversible species a self induced redox cycling occurs. The macroelectrode current is high however diffusion layer of microelectrode reaches only small portion of macroelectrode, therefore its current change is small an problematically measurable. Microelectrode current is substantially enhanced due to redox cycling between polarized microelectrode and polarized macroelectrode. Surprising results were obtained on the microelectrode while macroelectrode was disconnected from

bipotentiostat. Current on microelectrode is practically the same as measured with polarized macroelectrode.

The mechanism of self-induced redox cycling was explained by Horiuchi using combined twin chip with microdisc array electrode and macroelectrode with the same area [42]. The current on microdisc array electrode is higher as on the same microelectrode placed on chip without macroelectrode. Oxidized form produced on microdisc electrode diffuses to vicinity of macroelectrode and creates local concentration gradient (point A).

In the agreement of equilibrium establishing on macroelectrode surface, the opposite reaction is induced and in point B the same electrode reaction as on microdisc electrode. Reduced species generated on macroelectrode in point A diffuses back to microdisc electrode due to its concentration deficit at this location and oxidizes again closing redox cycle. Current enhancement grows with area of macroelectrode until it is hundred times greater than the area of microelectrode.

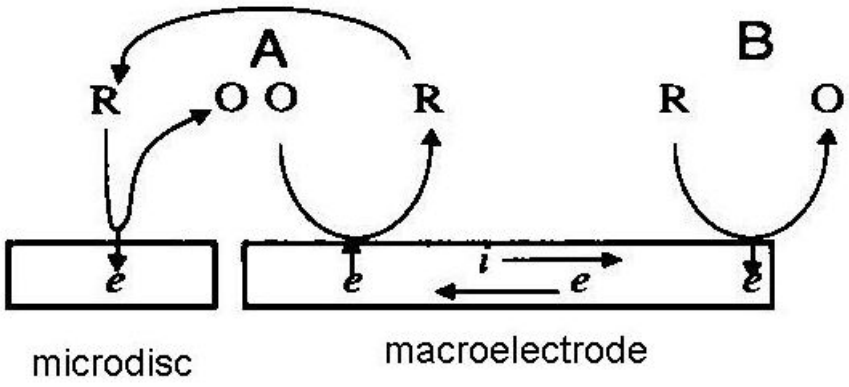

Fig. 5: *Mechanism of self induced redox cycling [42]*

Parameter for quantitative consideration of redox cycling is number of redox cycles. It was calculated from collection efficiencies. If collection efficiency in the direction from generator to the collector is Φ_1 and in the opposite direction from collector to the generator is equal to Φ_2 number of molecules of species obeying one electron electrode reaction diffusing on the collector is equal to $N\Phi_1$ and number of molecules diffusing back to the generator is therefore $N\Phi_1\Phi_2$ and number of molecules diffusing to the bulk phase of the solution is then equal $N - N\Phi_1\Phi_2$ where N is number of molecules oxidized per time unit on the generator. Based on these ideas number of redox cycles can be expressed as

$$R_C = \frac{N}{N(1-\Phi_1\Phi_2)} = \frac{1}{1-\Phi_1\Phi_2} \qquad (13)$$

Accuracy of parameter R_C depends on accuracies of determination of collection efficiencies in both directions however in the most of studies generator and collector were the same. Average number of redox cycles can be calculated also as current ratio of generator in dual mode I_g and in single mode I_0. Parameter I_g/I_0 is highly reproducible and may substitute values R_C calculated from equation (13) in the collection efficiencies range of 10-99%.

Fabrication of Microelectrode Arrays with Interacting Diffusion Layers

Microband electrodes (Fig.6) are the simplest type of microelectrode arrays with interacting diffusion layers. They were fabricated by placing insulating foil of width 2, 4 or 6 μm between Pt foil with width of 4 μm on a glass wafer [43]. The construction was improved by adding a small amount of epoxide on glass wafer and between all foils. The electrode surface was cleaned by sonization in a mixture of methanol and water. The electrode length was determined optically.

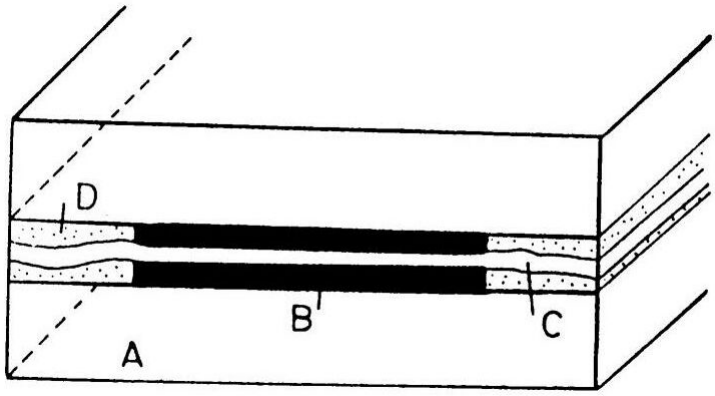

Fig. 6: *Double microband electrode: A-Glass, B-metal foil, C-spacer, D-epoxy [43].*

Ferocen in acetonitrile solution served as a testing redox system. Collection efficiency calculated as collector vs. generator current ratio was in the range of 10% to 50% and its value does not depend on ionic strength of the solution [44-46].

Very efficient fabrication technique for microelectrode arrays is photolithography widely used in book printing, gravure printing, offset techniques and microelectronics. The

most important field of photolithography is planar technology for the fabrication of planar microelectronic elements like integrated circuits etc. In this technique, a silicon wafer covered with a thin layer of silicon dioxide is used.

On this wafer, a continuous metal layer is placed and final shaping is performed by photolithographic etching. By using photoresists a horizontal relief is formed in dielectric and metal layers on the surface of silicon semiconductor. Photoresist species must be photosensitive and stable against aggressive etching agents. Electron resist are mostly used for microelectrode arrays fabrication because relief etching is performed by a flux of electrons, x-rays and reactive ions. Photoresist exposition is a diffusion process based on insolubility of cross-linked (illuminated) polymers. During photoresist exposition dark part of photoresist is dissolved in hot solution of the developer leaving uncovered parts of SiO_2 on wafer surface and illuminated (cross-linked) part of photoresist will remain.

Uncovered parts are etched by using photomask for obtaining desired geometrical shape. Finally, into etched places metal layer is incorporated [47-49]. For microelectrode arrays fabrication process are successfully used chemically cross-linked photoresists [50-53]. Their work is based on diffusion of acid protons catalyzing cross-linking process into resist. After exposition protons are reduced to H_2 and loose catalytic ability [54].

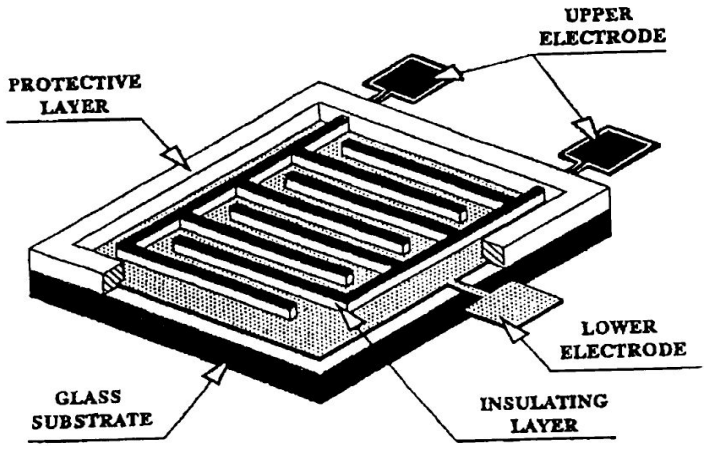

Fig. 7: *Horizontally separated IDA array with vertically separated lower macroelectrode [55].*

Horizontally (see Fig.7, above) and vertically (Fig.8, overleaf) separated IDA micro-electrodes were fabricated photolitographically. On thermally oxidized silicon wafer a layer of photoresist was placed and exposed by UV rays through the photomask then rinsed with deionized water followed by Pt film placing with width of 100 nm. Silicon dioxide film was etched with reactive ions in tetrafluoromethane [32,41]. During characterization five times

greater signal on vertically separated IDA array with a submicrometrical gap of 0.5 μm (R_C=35) was obtained in comparison with a planar IDA microelectrode (R_C=7) with gap of 2.5 μm corresponding to high level of redox cycling [41].

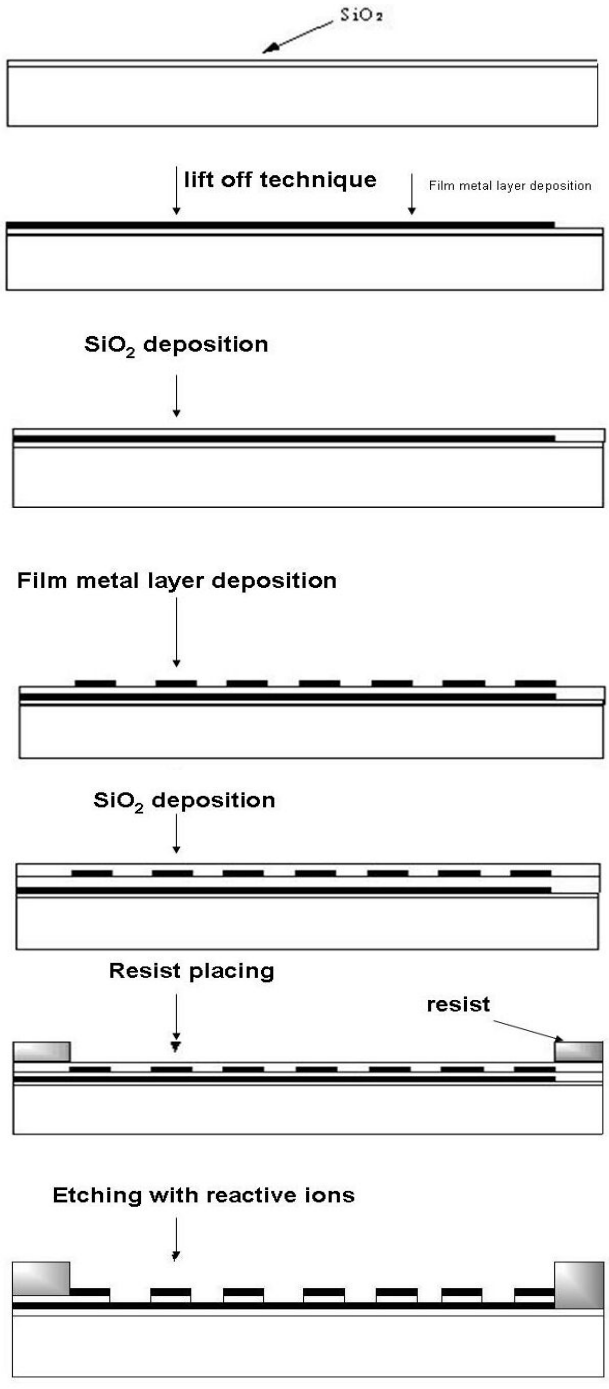

Fig. 8: *Scheme of vertically separated IDA array photolitographic fabrication [41].*

Anjo et al [56] showed that also carbon may serve as an electrode material for IDA microelectrodes fabrication. In ref. [57] vertically separated IDA microelectrodes with double layer of carbon and platinum are described. Fabrication of carbon film is based on pyrolysis

of 3,4,9,10-perylenetetracarboxylic acid dianhydride (PTCDA) according to Kaplan [58]. For the obtaining of carbon film with large area and the smooth surface, a slow evaporation of PTCDA is needed.

Temperature of pyrolysis is about 1000 ºC to assure good conductivity of carbon film. Structure of carbon film was checked by x-ray diffraction and Raman spectrometry. Cyclic voltammogram shows relatively high potential shift corresponding high IR drop. It may be decreased by using IDA microelectrode with combined microelectrode segments (one carbon and second platinum). High background current is caused by a high roughness of carbon film surface (average thickness of 5 nm)

Basic Electroanalytical Applications of Microelectrode Arrays with Interacting Diffusion Layers

Microelectrode arrays with interacting diffusion layers are very perspective tools in contemporary electroanalytical chemistry. They can be used as sensors for fast, sensitive and highly selective determination of species which are important in biology, food, medicine and the environment. Electroanalytical voltammetric techniques based on using microelectrode arrays with interacting diffusion layers utilize effects brought by a close geometrical arrangement of individually addressable segments in the array. Redox cycling on the adjacent segments is able to enhance current response what may increase the sensitivity.

The selectivity is enhanced by the fact that electrochemically irreversible redox pairs are not transferred on the collector [59]. Certain limitation represents usability only in the case of reversible or quasireversible charge transfer of the target species as well as the chip with a microelectrode array must be placed into non-aggressive media to avoid its damage. Save pH range showed to be from 3 to 11 ref. [60]. One way how to overcome these limitations is surface modification of microelectrode arrays with various polymeric films [61-63].

HPLC Detection with IDA Microelectrode

Short time response and current without capacity noise is utilized for amperometric detection of species in flow systems [64]. Amperometric detection in liquid chromatography is very popular in analysis of trace amounts of organic species due its high sensitivity, selectivity [65], in addition if microelectrode is used as amperometric detector, small amount of the supporting electrolyte is involved. In the 1980s and 1990s, a series of individually polarizable

electrodes started to be used for this type of analysis [66-68]. However, there was no overlap of diffusion layer due to its high distance between each other; hence, they were substituted by microelectrodes with close geometrical arrangement of individually fitted segments [69,70].

The simplest type of this kind of microelectrode arrays was double rectangular electrode (DRE) [71]. DRE has ability to enhance the selectivity of the detection when on one rectangle the interferents are irreversibly oxidized and chromatogram obtained on the second rectangle with potential more negative as on the first one does not contain peaks of irreversible interferents. This situation is practically equal also for IDA microelectrodes [72-74], however its geometry allows to reach substantially higher values of collection efficiency as well as higher level of redox cycling thus enhance current response [75-79]. This methodology is applied to selective detection of catecholamines [80-87].

Catecholamines are important biological compounds mediating a nerve perturbation in a synaptic cleft, therefore its sensitive and selective detection is needed. Biological samples contain a significant amount of interferents [88,89] such as l-ascorbic acid (AA), uric acid (UA) and catecholamines metabolites like dihydroxyphenylacetic acid (DOPAC) and homovanilic acid (HVA) so it is important to eliminate the influence of these interferents on the sensitivity and selectivity of catecholamines determination. Collection efficiencies for catecholamines are equal to 0.53-0.56 and collection efficiencies of interferents are practically equal to zero due to their electrochemical irreversibility. Consequently, peaks of catecholamines will become dominant in a chromatogram recorded at the collector. It was observed that steady-state current on IDA microelectrode in dual mode depends on cubic root of flow rate. This fact is caused by redox cycling [90-92]. When IDA microelectrode with a gap around of 1μm is used its response is not dependent on flow rate [93, 94].

Further improvement of detection limit of the determination of catecholamines brings carbon IDA microelectrode arrays [95-99]. Before measurement carbon IDA microelectrode must be electrochemically pretreated to assure reversible response of catecholamines [100-103], however capacity current is increased and potential window will become narrower after pretreatment [104,105]. If carbon IDA electrode with some hundreds of generator-collector pairs segments is used collection efficiency for catecholamines may increase to 70%. Due to high level of redox cycling and hence high signal to noise ratio detection limit around 10^{-11} mol.dm^{-3} may be reached. It corresponds 5 fg resp. 32 amol of dopamine (absolute amount) [106, 107].

IDA microelectrodes remove disadvantages of classical electrochemical detection as reactions of several species on the electrode [108] and high background current.

Electrochemical detection is faster than fluorescence detection based on the derivatization with 1,2-diphenylenediamine (DPE) which involves long reaction time [109-111] and other operations [112] as well as chemiluminiscence detection [113-115].

Another approach in the selectivity improvement of the determination of catecholamines represents electrochemical cells with a small volume. Microcells are constructed by a lithographic placing of the sensor with 50 pairs of the segment with a width of 3μm and 2 or 5 μm gap distance onto silicon wafer together with reference and counter microelectrodes (Fig.9) [116]. Ascorbic acid was used as interferent. The selectivity of the sensor was tested on 4 ml macrocell and 2μl microcell. Model sample contained dopamine with a concentration of 1×10^{-4} mol.dm^{-3} and ascorbic acid of the concentration 1×10^{-3} mol.dm^{-3}.

Results were compared with dopamine signal without interferent (Fig. 10). Anodic current in a macrocell with an addition of ascorbic acid is very high corresponding its irreversible oxidation. Anodic current in a microvolume cell is also high, however in certain time it reaches the current value of the sample without ascorbic acid due to its bulk phase (coulometric) oxidation because sensor and sample volume have comparable dimensions.

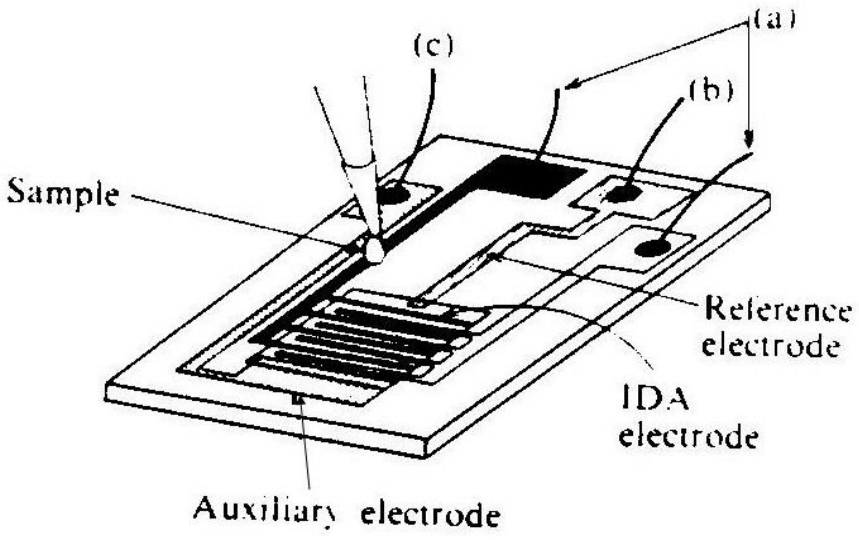

Fig. 9: *Small volume IDA electrochemical microcell [116]:* **a**-contacts for IDA micro-electrodes, **b**-contact for reference electrode, and **c**-contact for counter electrode.

A lowering of the analyzed volume increases the selectivity of electrochemical detection of catecholamines. Collection efficiency of dopamine on the concentration of ascorbic acid was investigated. It was shown in the case of macrocell decreasing of the

collection efficiency when concentration of ascorbic acid is increased. However collection efficiency in microvolume cell remains stable around more than 50% even concentration of ascorbic acid is 30 times higher than the concentration of dopamine [116,117].

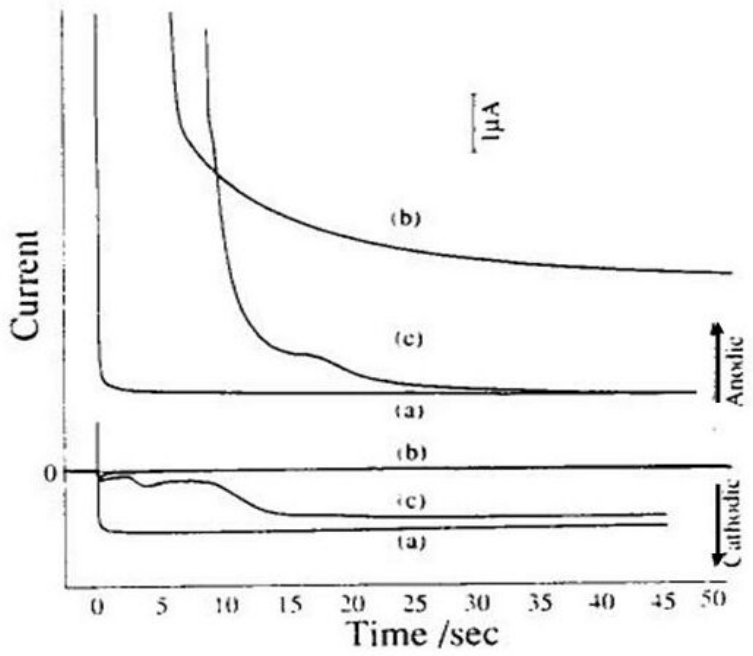

Fig. 10: *Chronoamperograms of 1×10^{-4} mol.dm^{-3} dopamine with and without 1×10^{-3} mol.dm^{-3} ascorbic acid [116].* (a) 4 ml cell dopamine without ascorbic acid (b) 4 ml cell dopamine with ascorbic acid, (c) 2μl cell dopamine with ascorbic acid.

Electrochemical Stripping Analysis of Reversible Redox Species with Self Induced Redox Cycling

The lowest detection limit from all electroanalytical techniques has electrochemical stripping analysis [118-120]. It is widely used for determination of metal ions and halides in water, food, biological fluids and environmental samples [121-123]. Detection limit of electrochemical stripping analysis is usually found in order of 10^{-10}-10^{-11} mol.dm^{-3} [124-126]. However this technique can be applied just for certain species such as metal ions, halides or adsorptive organic compounds by using special techniques as chemical modification of the working electrode surface or adsorptive complexes formation [127-131].

The so-called substitutional stripping voltammetry employing interdigitated micro-electrode array as the working electrode extends usability of stripping analysis also for species for which deposition onto electrode surface is not possible due to various reasons. The

common reason is the solubility of both forms of the target redox analyte. Substitutional stripping voltammetry (SSV) allows also detection of reversible species which has both forms of redox system well soluble.

The self-induced redox cycling described via explaining the interaction of diffusion layers of two closely spaced electrodes may also be realized in the double compartment cell (see Fig. 11 below and ref. [132]).

In this experimental arrangement a pair of individually addressable microelectrode segments forming IDA microelectrode is placed in the first compartment and macroelectrode in the second one. One of pair of microelectrodes is connected with macroelectrode. In this system a charge produced by self induced redox cycling in the first compartment is transferred into another electrochemical reaction in the second compartment.

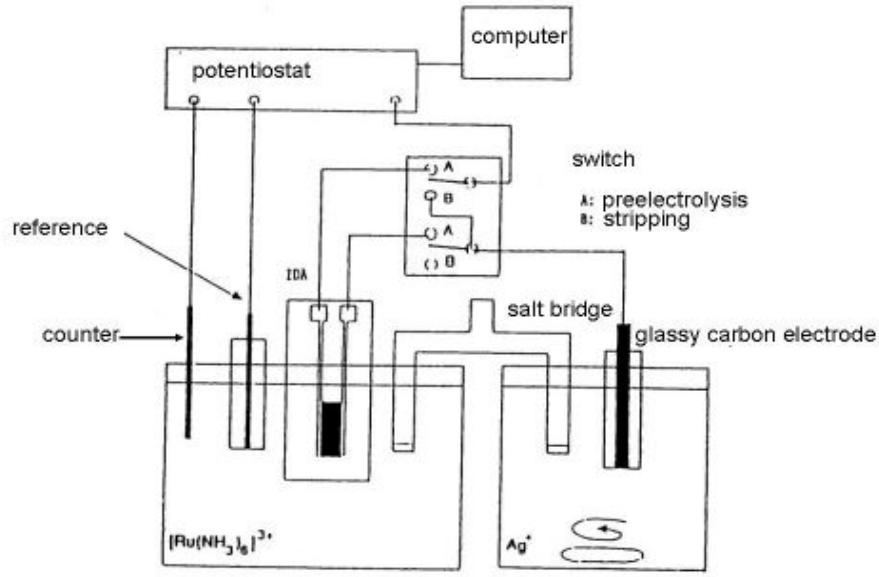

Fig. 11: *SSV measuring system scheme* (after [74])

In the case depicted in Fig 11, an oxidized form of reversible redox system is analyzed. Redox cycling in first (left) compartment may induce in the second (right) compartment deposition of substitutional compound as solid species onto macroelectrode surface [132,133]. This process is called preelectrolysis and its duration depends on operator. Amount of substitutional species is determined by its stripping like in a classic voltammetric stripping analysis (Fig. 12). Amount of substitutional species is proportional to the concentration of oxidized form of target species in first compartment and a stripping peak is then suitable for its quantification [74]. The term substitutional stripping voltammetry is derived from a fact

that during preelectrolysis substitutional species in the second compartment of the measuring system is deposited and stripped instead of analyzed reversible species with both redox form soluble in the solvent [133].

Substitutional stripping voltammetry has two variants. The first one is cathodic SSV in which the analyzed species is ferrocenylmethyltrimethylammonium bromide (aq-ferrocene) [133]. As a substitutional electrolyte iodide was used together with silver electrode in the second compartment. During preelectrolysis, AgI is deposited onto silver electrode surface offering a stripping peak at the potential of -0.2V vs. SCE. Potential of left electrode was fixed at 0.55V vs. SCE corresponding to the limiting current of the oxidation to aq-ferricene. The silver electrode was polarized by a scan in the range of 0.25 to -0.4V vs.SCE during the stripping step.

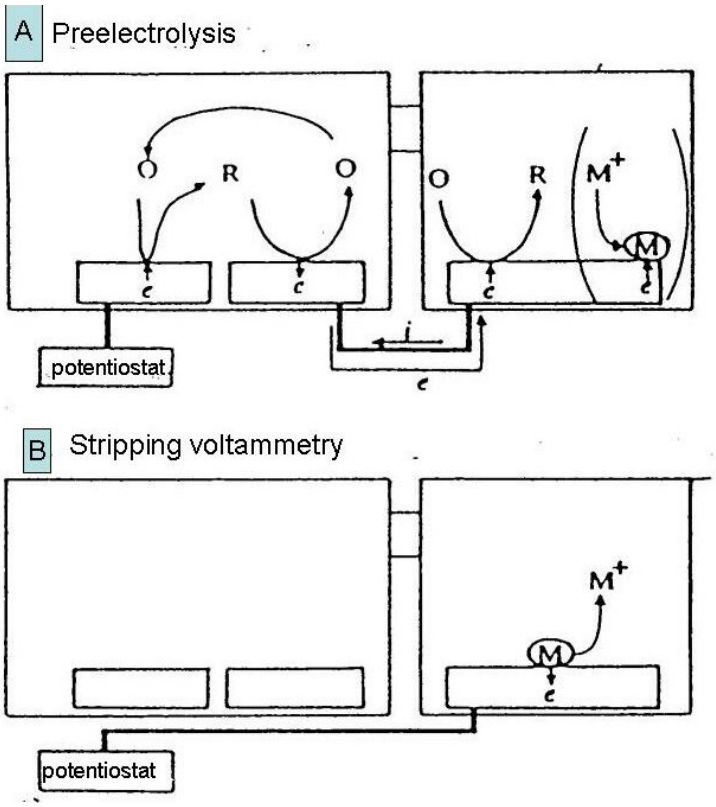

Fig. 12: *Principle of substitutional stripping analysis* (after [132]). A- transfer of redox cycling to the right compartment during preelectrolysis step. B- electrochemical stripping of metal deposited on macroelectrode.

If the concentration of iodide is equal to 1×10^{-6} mol.dm^{-3} stripping peak height is proportional to the preelectrolysis time and no stripping peak was observed in the absence aq-ferrocene. However by the comparison of charge passed during redox cycling with

stripping charge of AgI it was observed that coulombic efficiency of charge transfer between two compartments is only 3.2%. This value is too low for high sensitivity assuring. By enhancing of iodide concentration to 1×10^{-5} mol.dm^{-3} practically 100% coulombic efficiency was achieved, however small stripping peaks of AgI was observed even no aq-ferrocene is present in the first compartment because at this higher concentration of iodide deposition in second compartment is induced by residual current at potential of 0.55V vs. SCE in the first compartment. Approximately 500 times greater signal was observed as for cyclic voltammetry.

Anodic SSV is based on the redox cycling of hexaamminruthenium(III) chloride [133]. It is oxidized form of typically reversible redox system with a reduction potential of -0.2V vs. SCE, therefore current flows in an opposite direction than in the case of aq-ferrocene. When this species is reduced on one segment of IDA array on the second segment it is oxidized and silver ions are deposited on glassy carbon electrode [134]. Then the silver is anodically stripped in a positive sweep of the potential.

Fig. 11 depicts experimental arrangement for anodic SSV. It allows by using a switch in a position A polarize left segment of IDA array working microelectrode with a constant potential of -0.4V vs. SCE. At this potential reduction $[Ru(NH_3)_6]^{3+}$ to $[Ru(NH_3)_6]^{2+}$ proceeds with limiting current. Right segment of IDA array is connected with glassy carbon electrode in the second compartment of electrolytic cell. During preelectrolysis redox cycling of $[Ru(NH_3)_6]^{3+}$ is transferred to the deposition of AgI on glassy carbon electrode in a stirred solution. After preelectrolysis time (typically 10 min.) the switch is turned to position B and solution is stabilized during quiet conditions for 10 s. Then the potential of glassy carbon electrode is scanned from -0.4 to +0.5V vs. SCE with a scan rate of 20 mV.s^{-1}. Stripping peak of silver was found at +0.35V vs. SCE. No peak was observed at the potential lower than -0.4V or when no $[Ru(NH_3)_6]^{3+}$ was present in a solution in the first compartment [132]. Cyclic voltammogram on the left segment of IDA array was measured and compared with an oxidation current on right segment of IDA. There was observed no significant difference indicating high collection efficiency, but oxidation current contained substantially small portion of signal of interferences. This fundamental decreasing of background signal is base for preelectrolysis to assure high signal to noise ratio achieving such high sensitivity also for stripping peak. By comparison of cyclic voltammogram with redox cycling and silver stripping peak approximately 80 times greater signal was obtained however this signal is 2500 time higher than one obtained by simple cyclic voltammetry.

Otherwise, coulombic efficiency of transfer oxidation of $[Ru(NH_3)_6]^{3+}$ to silver stripping was only around 43%. Detection limit was estimated to 1×10^{-8} mol.dm^{-3} and linear

dynamic concentration range was from 1×10^{-8} to 1×10^{-7} mol.dm^{-3}. Linearity was disappeared when concentration of $[Ru(NH_3)_6]^{3+}$ was increased to 1×10^{-6} mol.dm^{-3} [132] due to decreasing of coulombic efficiency.

As macroelectrode material for the deposition of silver ions glassy carbon was used. GC electrode has wide potential window and charge transfer between silver ions and its surface is reversible. Another electrodes e.g. hanging mercury electrode are also suitable for using in SSV experiments, however potential window is narrower especially in an anodic potential range limiting thus stripping potential sweeping. For assuring sufficient deposition rate needed for charge consumption generated by redox cycling are suitable silver ions, Hg^{2+} ions are also suitable because their potential is sufficiently higher as the potential of $[Ru(NH_3)_6]^{3+}$ oxidation. Some limitations may occur if various anions forming complexes with Hg^{2+} are present in a solution [134].

Further important parameters to be optimized are: macroelectrode area, concentration of substitutional species and scan rate during stripping step. When the concentration of analyzed species is low, signal to noise ratio is also low and very small amount of Ag^+ ions is deposited on macroelectrode. In addition, faradayic and capacity current of various impurities remains stable therefore it is difficult to obtain baseline on big macroelectrode. It looks to be optimal when glassy carbon electrode with a diameter of 1 mm is used as macroelectrode for the deposition of substitutional species. Concentration of Ag^+ is also an important factor for decreasing of SSV detection limit. When concentration of Ag^+ is lower or the same as concentration of analyzed species in the first compartment, coulombic efficiency is substantially lower than 100%, because deposition of silver ion will become rate determinatig step and the whole charge produced by redox cycling during preelectrolysis cannot be transferred on the Ag^+ deposition. Coulombic efficiency is near 100% when Ag^+ concentration is at least one order greater than the concentration of $[Ru(NH_3)_6]^{3+}$.

Similar results were obtained for cathodic SSV for iodide as substitutional species and aq-ferrocene as analyte. Scan rate during stripping step is also an important parameter for for reliability of SSV determinations. High scan rate produces high stripping peak with a biased baseline and it is difficult to dissolve all silver with linear sweep of the potential [135]. Otherwise low scan rate causes underpotential deposition of silver [136]. For both limitations is satisfactory value of 20 mV.s^{-1}. Starting potential for stripping is usually set up to to the potential of generator (left) segment of IDA array. Higher potential is also possible, however in this case current caused by switch turning from preelectrolysis mode to stripping mode may

affect stripping peak. This current does not occur if potential of generator segment of IDA array and starting potential of stripping sweep are equal.

On Fig. 13a are depicted SSV voltammograms of 1×10^{-11} mol.dm^{-3} $[Ru(NH_3)_6]^{3+}$ for various times of preelectrolysis. Voltammograms on Fig. 13b was obtained under the same conditions as Fig. 13a, but without $[Ru(NH_3)_6]^{3+}$ Stripping peaks of silver was observed at potential of 0.3V vs. SCE and they are dependent on preelectrolysis time and no peaks was obtained in no presence of $[Ru(NH_3)_6]^{3+}$. This shows that electrolysis of $[Ru(NH_3)_6]^{3+}$ causes deposition of silver ions [133].

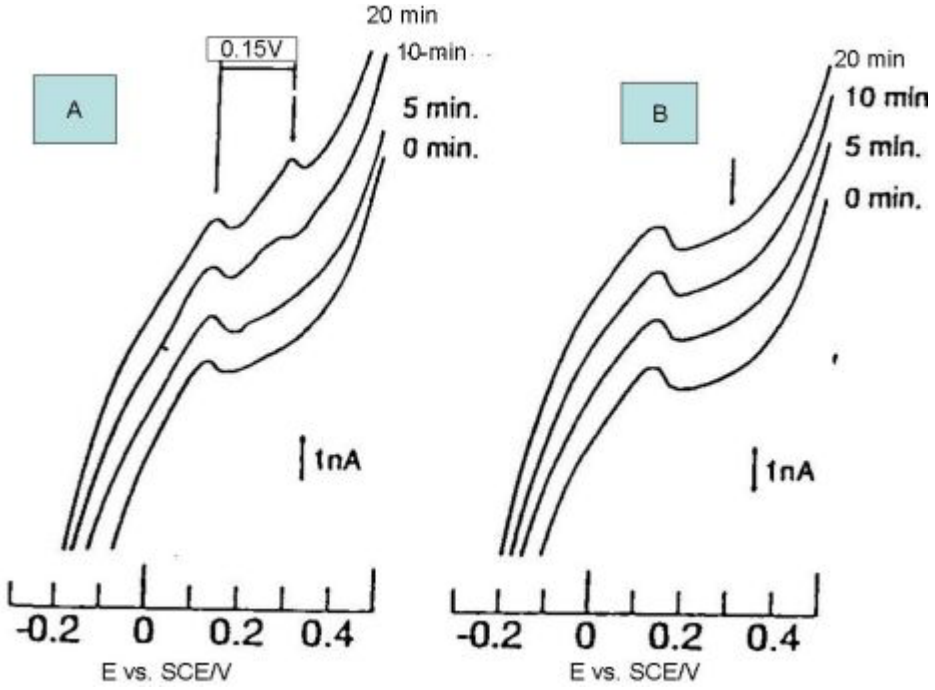

Fig. 13: *Substitutional stripping voltammograms* (taken from [75]). Concentration of Ag^+ as substitutional electrolyte was 1×10^{-7} mol.dm^{-3}. **A**- 1×10^{-11} mol.dm^{-3} $[Ru(NH_3)_6]^{3+}$; **B**- no $[Ru(NH_3)_6]^{3+}$

Peak height after 20 min preelectrolysis was around 0.5 nA. Theoretical value of the limiting current of the $[Ru(NH_3)_6]^{3+}$ solution with a concentration of 1×10^{-11} mol.dm^{-3} in dual mode for IDA microelectrode was 0.8 pA [133]. SSV signal is 630 times higher. Peak area was 1.1 nC. Charge passed during preelectrolysis was 0.96 nC, therefore coulombic efficiency is 115%. 15% deviation may be caused by dissolved oxygen. Oxygen was removed before preelectrolysis by bubbling with pure nitrogen, however it is impossible to bubble solution

during preelectrolysis because redox cycling is very sensitive to convection. Small amount of oxygen is able to dissolve in a solution during 20 min preelectrolysis.

Concluding, SSV is suitable electroanalytical technique for the detection of reversible redox species of very low concentrations. The current from the collector segment of IDA array can be integrated because it has a small content of background signal. The integration may be performed by coulometer however its resistivity may interfere with redox cycling.
In SSV experiments, the direct connection of electrodes in various compartments minimizing internal resistivity and macroelectrode behaves as ideal chemical coulometer. SSV was successfully applied to the detection of dopamine. If IDA microelectrode is used in dual mode detection limit of 1×10^{-8} mol.dm^{-3} was obtained. In SSV experiments silver macroelectrode and iodide were used for substitutional stripping. After optimization of measuring conditions a cathodic stripping peak dependent on preelectrolysis time and concentration of dopamine was observed.

It was shown that it is possible to detect dopamine on concentration level of 1×10^{-9} mol.dm^{-3}. This detection limit is low than on IDA electrode in dual mode, but substantially higher as for the detection of $[Ru(NH_3)_6]^{3+}$ because detection limit of AgI stripping is about 1-2 orders higher than anodic stripping of silver. One possibility how to increase sensitivity of substitutional stripping of dopamine is applying of gold IDA microelectrode or carbon IDA microelectrode with quasi reversible charge transfer of dopamine [137].

Conclusions

In this chapter microlithographically fabricated microelectrodes and their array are described. These powerful electroanalytical tools can be used as very sensitive and selective detectors hyphenated with separation analytical techniques. They may to recognize signals of irreversible redox systems from reversible redox species due to redox cycling in dual mode at two adjacent microelectrodes polarized with various potentials corresponding direct and opposite electrochemical reaction taking place in electrochemical systems.

Microelectrode arrays may be also used for stripping analysis of species which cannot be deposited onto electrode surface as solid species because its natural solubility in a solvent. Redox cycling is possible to transfer to another compartment of electrolytical cell inducing deposition process of substitutional species.

Acknowledgements

Financial support from Scientific Grant Agency of Slovak Republic (project VEGA 1/0008/12) is gratefully acknowledged.

References

1. R. M. Wightman: *Science* **240** (1988) 415.
2. J. O. Howell, R. M. Wightman: *Anal. Chem*. **56** (1984) 524.
3. D. C. Johnson, M. D. Ryan, G. S. Wilson: *Anal. Chem*. **60** (1988) 147R.
4. H. Reller, E. Kirowa - Eisner, E. Gileady: *J. Electroanal. Chem*. **161** (1984) 247.
5. J. A.Wise, W. R. Heineman, P. T. Kissinger: *Anal. Chim. Acta* **172** (1985) 1.
6. F. Vydra, K. Štulík, E. Juláková : *Rozpouštecí polarografie a voltametrie.* Praha , SNTL , (1977).
7. W. T. De Vries, E. van Dalen: *J. Electroanal. Chem.* **14** (1967) 315.
8. M. A. Dayton, J. C. Brown, K. J. Stutts, R. M. Wightman: *Anal. Chem*. **52** (1980) 946.
9. J . Wang: *Stripping Analysis.*, Inc. Deerfield Beach, Florida VCH Publishers (1985).
10. P. Tomčík, D. Bustin: *Fres. J. Anal. Chem*. **371** (2001) 562.
11. T. M. Florence: *J. Electroanal. Chem*. **27** (1970) 273.
12. G. Hills, A. K Pour., B. Scharifker: *Electrochim. Acta* **28** (1983) 891.
13. B. Scharifker, G. Hills: *J. Electroanal. Chem*. **130** (1981) 81.
14. G. Gunawardena, G. Hills, B. Scharifker: *J. Electroanal. Chem.* **130** (1981) 99.
15. G.J. Hills, D.J. Schiffrin, J. Thompson: *Electrochim. Acta* **19** (1974) 657.
16. G. Gunawardena, G.J. Hills, I. Montenegro: *Electrochim. Acta* **23** (1978) 693.
17. M.R. Cushman, B.G. Bennet, C.W. Anderson: *Anal.Chim Acta* **130** (1981) 323.
18. K. Aoki, K. Tokuda, H. Matsuda: *J. Electroanal. Chem*. **235** (1987) 87.
19. A.M Bond, K.B. Oldham, C.G. Zoski: *J. Electroanal. Chem*. **245** (1988) 71.
20. C. G. Zoski, A.M. Bond, E.T. Alinson, K.B. Oldham: *Anal. Chem*. **62** (1990) 37.
21. K. Aoki, K. Honda, K. Tokuda, H. Matsuda: *J. Electroanal. Chem.* **182** (1985) 267.
22. C. Amatore, M.R. Deakin, R. M Wightman: *J. Electroanal. Chem*. **206** (1986) 23.
23. K. Aoki, K. Honda, K. Tokuda, H. Matsuda: *J. Electroanal. Chem*. **195** (1985) 51.
24. K. Aoki, H. Kaneko: *J. Electroanal. Chem*. **247** (1988) 17.
25. K. Aoki, M. Tanaka: *J. Electroanal. Chem.* **266** (1989) 11.

26. H.A.O. Hill, N.A. Klein, I.S.M. Psalti, N.J. Walton: *Anal. Chem*. **61** (1989) 2200.
27. K. Aoki: *J. Electroanal. Chem*. **270** (1989) 35.
28. H. Ju, H. Chen, G. Hong: *J Electroanal. Chem*. **341** (1992) 35.
29. K. Aoki, K. Tokuda, H. Matsuda: *J. Electroanal. Chem*. **225** (1987) 19.
30. K. Aoki, K. Tokuda: *J. Electroanal. Chem.* **237** (1987) 163.
31. A. Szabo, D. K. Cope, D. E.Tallmann, P. M Kovach, R. M. Wightman: *J. Electroanal. Chem.* **217** (1987) 417.
32. D. E. Weisshaar, D.E. Tallman: *Anal. Chem.* **55** (1983) 1146.
33. H. Matsuda, K. Aoki, K. Tokuda: *J. Electroanal. Chem.* **217** (1987) 15.
34. K. Aoki, K. Tokuda, H. Matsuda: *J. Electroanal. Chem.* **230** (1987) 61.
35. S. Coen, D. K. Cope, D.E. Tallman: *J. Electroanal. Chem.* **215** (1986) 29.
36. A. J. Bard, J. A. Crayston, G. P. Kittlesen, T. V. Shea, M. S. Wrighton: *Anal. Chem*. **58** (1986) 2321.
37. O. Niwa, M. Morita, H. Tabei: *Anal. Chem*. **62** (1990) 447.
38. P. Tomčík, Š Mesároš, D. Bustin: *Anal. Chim. Acta* **374** (1998) 283.
39. P. Tomčík, D. Bustin, I. Novotný: *Chem. Listy* **95** (2001) 18.
40. P. Tomčík, P. Jenčušová, M. Krajčíková, D. Bustin, R. Brescher: *Anal. Bioanal. Chem*. **383** (2005) 864.
41. D. Bustin, Š. Mesároš, P. Tomčík, M. Rievaj, V. Tvarožek: *Anal. Chim. Acta* **305** (1995) 121.
42. T. Horiuchi, O. Niwa, M. Morita, H. Tabei: *J. Electrochem. Soc.* **138** (1991) 3549.
43. J. E. Bartelt, M. R. Deakin, C. Amatore, R. M. Wightman: *Anal. Chem*. **60** (1988) 2167.
44. A. M. Bond, T. L. E. Henderson, W. Thormann: *J. Phys. Chem*. **90** (1986) 2911.
45. W. Thormann, P. van den Bosch, A. M. Bond: *Anal. Chem*. **57** (1985) 2764.
46. B. J. Seddon, H.H. Girauld, M. J. Edoves: *J. Electroanal. Chem*. **293** (1990) 269.
47. W. E. Geiger, D.E. Smith: *J. Electroanal. Chem*. **50** (1974) 31.
48. K. Aoki, M. Morita, O. Niwa, H. Tabei: *J. Electroanal. Chem*. **256** (1988) 269.
49. O. Niwa, M. Morita, H. Tabei: *J. Electroanal. Chem. Interfacial Electrochem*. **267** (1989) 291.
50. K. Aoki, K. Honda, K. Tokuda, H. Matsuda: *J. Electroanal. Chem* **186** (1986) 79.
51. H. Ban, J. Nakamura, K. Deguchi, A. Tanaka: *J. Vac. Sci. Technol. B* **9** (1991) 3387.
52. H. Ito, C. G. Willson: *Polym. Eng. Sci.* **23** (1983) 1012.
53. H. Liu, M.P. de Grandpre, W. E. Feely: *J. Vac. Sci. & Technol. B* **6** (1988) 379.

54. J. Nakamura, H. Ban, M. Morita, A. Tanaka: *Jpn. J. Appl. Phys.* **32** (1993) L813.
55. J. Polonský, M. Rievaj, D. Bustin: *Chem. Anal. (Warsaw)* **42** (1997) 445.
56. A. Rojo, A. Rosenstratten, D. Anjo: *Anal. Chem*. **58** (1986) 2988.
57. H. Tabei, M. Morita, O. Niwa, T. Horiuchi: *J. Electroanal. Chem*. **334** (1992) 25.
58. M. L. Kaplan, P.H. Schmidt, C. H. Chen, W. M. Walsh: *Appl. Phys. Lett*. **36** (1980) 867.
59. P. Tomčík, D. Bustin, V. Tvarožek: *Chem. Listy* **93** (1999) 678.
60. P. Tomčík, L. Mrafková, D. Bustin: *Microchim. Acta* **141** (2003) 69.
61. H. S. White, G. P. Kittlesen, M. S. Wrighton: *J. Am. Chem. Soc*. **106** (1984) 5375.
62. G. P. Kittlesen, H. S. White, M.S. Wrighton: *J. Am. Chem. Soc*. **106** (1984) 7389.
63. G. P. Kittlesen, H. S. White, M. S. Wrighton: *J. Am. Chem. Soc.* **107** (1985) 7373.
64. C. E. Lunte, P. T. Kissinger, R. E. Shoup: *Anal. Chem*. **57** (1985) 1541.
65. T. Matsue, A. Aoki, I. Uchida: *Redox Chemistry and Interfacial Behavior of Biological Molecules* , Plenum , New York, (1988).**457**
66. D. A. Roston, R. E. Shoup, P. T. Kissinger: *Anal. Chem*. **54** (1982) 1417A.
67. T. V. Shea, A. J. Bard: *Anal. Chem.* **59** (1987) 2101.
68. D. Belanger, M.S. Wrighton: *Anal. Chem.* **59** (1987) 1426.
69. T. Matsue, A. Aoki, E. Ando, I. Uchida: *Anal. Chem*. **62** (1990) 407.
70. L. E. Fosdick, J. L. Anderson: *Anal. Chem*. **58** (1986) 2481.
71. P.C Johnson, S. G. Weber, R. M. Wightman, R. E Shoup, I. S. Krull: *Anal. Chim. Acta* **180** (1986) 187.
72. S. Moldoveanu, J. L. Anderson: *J. Electroanal. Chem. Interfacial Electrochem*. **185** (1985) 239.
73. V. Y. Filinovsky: *Electrochim. Acta* **25** (1980) 309.
74. D. K. Cope, D.E. Tallman: *J. Electroanal. Chem. Interfacial Electrochem*. **188** (1985) 21.
75. J. L. Anderson, T. Y. Ou, S. Moldoveanu: *J. Electroanal. Chem. Interfacial Electrochem*. **196** (1985) 213.
76. T. Y. Ou, S. Moldoveanu, J. L. Anderson: *J. Electroanal. Chem. Interfacial Electrochem*. **247** (1988) 1.
77. T. Hepel, J. Osteryoung: *J. Electrochem. Soc.* **133** (1986) 752.
78. T. Matsue, A. Aoki, T. Abe, I. Uchida: *Chem. Lett*. **1** (1989) 133.
79. M. Takahashi, M. Morita, O. Niwa, H. Tabei: *J. Electroanal. Chem*. **335** (1992) 253.
80. T. Matsue: *Trends Anal. Chem*. **12** (1993) 100.

81. J. W. Bixler, A. M. Bond: *Anal. Chem.* **58** (1986) 2859.
82. S. B. Khoo, H. Gunasingham, K. P. Ang, B. T. Tay: *J. Electroanal. Chem.* **216** (1987) 115.
83. D. C. Johnson, W. R. Lacourse: *Anal. Chem.* **62** (1990) A589.
84. W. L. Caudill, J. O. Howell, R. M. Wightman: *Anal. Chem*. **54** (1982) 2532.
85. L. J. Magee, J. Osteryoung: *Anal. Chem.* **62** (1990) 2625.
86. R. S. Stojanovic, A. M. Bond, E. C. V. Butler: *Anal. Chem.* **62** (1990) 2692.
87. A. Aoki, T. Matsue, I. Uchida: *Anal. Chem.* **62** (1990) 2206.
88. R. N. Adams: *Anal. Chem.* **48** (1976) 1126A.
89. R. M. Wightman, L. J. May, A. C. Michael: *Anal. Chem.* **60** (1988) 769A.
90. L. J. May, W. G. Kuhr, R. M. Wightman: *J. Neurochem.* **51** (1988) 1060.
91. S. G. Weber: *J. Electroanal. Chem. Interfacial Electrochem.* **145** (1983) 1.
92. F. A. Posey, R.E. Meyer: *J. Electroanal. Chem. Interfacial Electrochem.* **30** (1971) 359.
93. S. G. Weber, W. C. Purdy: *Anal. Chim. Acta* **100** (1978) 531.
94. K. Aoki, K. Tokuda, H. Matsuda:
J. Electroanal. Chem. Interfacial Electrochem. **217** (1987) 33.
95. O. Niwa, H. Tabei: *Anal. Chem.* **66** (1994) 285.
96. O. Niwa, M. Morita: *Anal. Chem.* **68** (1996) 355.
97. G. Sreenivas, S. S. Ang, J. Fritsch, W. D. Brown, G. A. Gerhardt, D. J. Woodward:
Anal. Chem. **68** (1996) 1858.
98. H. Tabei, M. Takahashi, S. Hosino, O. Niwa, T. Horiuchi:
Anal.chem. **66** (1994) 3500.
99. O. Niwa, H. Tabei, B. P. Solomon, F. M. Xie, P. T. Kissinger:
Journal of Chromatography B **670** (1995) 21.
100. A. G. Ewing, M. A. Dayton, R. M. Wightman: *Anal.Chem.* **53** (1981) 1842.
101. R. A. Saraceno, A. G. Ewing: *Anal. Chem*. **60** (1988) 2016.
102. J. L. Ponchon, R. Cespuglio, F. Gonon, M. Jouvet, J. F. Pujol: *Anal. Chem.* **51** (1979) 1483.
103. F. Gonon, M. Buda, R. Cespuglio: *Nature* **286** (1980) 902.
104. M. Poon, R. L. McCreery: *Anal. Chem.* **58** (1986) 2745.
105. H. Zhang, L. A. Coury Jr.: *Anal. Chem.* **65** (1993) 1552.
106. O. Niwa: *Bull. Chem. Soc. Jpn*. **78** (2005) 555.
107. O. Niwa, M. Morita, B. P. Solomon, P. T. Kissinger: *Electroanalysis* **8** (1996) 427.
108. J. Kehr: *J. Chromatogr.* **661** (1994) 137.
109. A. Mitsui, H. Nohta, Y. Ohkura: *J. Chromatogr*. **344** (1985) 61.

110. M. Lee, H. Nohta, Y. Ohkura: *J. Chromatogr.* B **378** (1986) 329.
111. M. K. Lee, H. Nohta, Y. Ohkura: *J. Chromatogr.* B **421** (1987) 237.
112. H. Nohta, E. Yamaguchi, Y. Ohkura, H. Watanabe: *J. Chromatogr. B* **493** (1989) 15.
113. G. Mellbin: *J. Liq. Chromatogr.* **6** (1983) 1603.
114. S. Kobayashi, J. Sekino, K. Honda, K. Imai: *Anal. Biochem.* **112** (1981) 99.
115. S. Higashidate, K. Imai: *Analyst* **117** (1992) 1863.
116. O. Niwa, M. Morita, H. Tabei: *Sens. Actuators B* **13 – 14** (1993) 558.
117. M. Morita, M. L. Longmire, R. W. Murray: *Anal. Chem*. **60** (1988) 2770.
118. T. M. Florence: *J. Electroanal. Chem. Interfacial Electrochem.* **35** (1972) 237.
119. T. M. Florence: *Anal. Chim. Acta* **141** (1982) 73.
120. J. L. Anderson, D. Jagner, M. Josefson: *Anal Chem.* **54** (1982) 1371.
121. R. S. Sadana: *Anal. Chem.* **55** (1983) 304.
122. J. T. Kinard: *Anal. Lett.* **10** (1977) 1147.
123. A. Hu, R. E. Dessy, A. Graneli: *Anal. Chem*. **55** (1983) 320.
124. M. Rievaj, P. Tomčík, Z. Jánošíková, D. Bustin, R. G. Compton: *Chemia Analityczna (Warsaw) **53*** (2008) 153.
125. P. Figura: *Anal. Chem*. **51** (1979) 120.
126. C. M. G. van den Berg: *Anal. Chim. Acta*. **164** (1984) 195.
127. C. M. G. van den Berg, G. S. Jacinto: *Anal. Chim. Acta*. **211** (1988) 129.
128. J. Wang, K. Varughese: *Anal. Chim Acta* **199** (1987) 185.
129. J. Wang, P. A. M. Farias, J. S. Mahmoud: *Anal. Chim. Acta* **171** (1985) 215.
130. C. M. G. van den Berg: *Analyst* **114** (1989) 1527.
131. J. C. Moreira, R. Zhao, A. G. Fogg: *Analyst* **115** (1990) 1561.
132. T. Horiuchi, O. Niwa, M. Morita, H. Tabei: *Anal. Chem*. **64** (1992) 3206.
133. T. Horiuchi, O. Niwa, M. Morita, H. Tabei: *Denki Kagaku* **60** (1992) 1130.
134. T. Horiuchi, O. Niwa, H. Tabei: *Anal. Chem*. **66** (1994) 1224.
135. D. M. Kolb, M. Przasnysky, H. Gerischer: *J. Electroanal. Chem*. **54** (1974) 25.
136. I. Morcos: *J. Electroanal. Chem*. **66** (1975) 250.
137. O. Niwa, M. Morita, H. Tabei: *Electroanalysis* **3** (1991) 163.